

# Nonconventional production technologies for NiTi shape memory alloys

F. Neves<sup>1,2,a</sup>, F.M. Braz Fernandes<sup>1</sup>, I. Martins<sup>2</sup>, J.B. Correia<sup>2</sup>, M. Oliveira<sup>2</sup>, E. Gaffet<sup>3</sup>, T.-Y. Wang<sup>4</sup>, M. Lattmann<sup>5,6</sup>, J. Suffner<sup>5,6</sup> and H. Hahn<sup>5,6</sup>

<sup>1</sup> CENIMAT/I3N, Faculdade de Ciências e Tecnologia, Universidade Nova de Lisboa, 2829-516 Caparica, Portugal

<sup>2</sup> LNEG, Laboratório Nacional de Energia e Geologia, Estrada do Paço do Lumiar, 22, 1649-038 Lisboa, Portugal

<sup>3</sup> NRG, UMR 5060 CNRS, UTBM, Site de Sévenans, F90010 - Belfort, France

<sup>4</sup> AKCMM, The University of Sydney, NSW, Sydney 2006, Australia

<sup>5</sup> Joint Research Lab Nanomaterials, TUD-FZK, 64287 Darmstadt, Germany

<sup>6</sup> INT, Forschungszentrum Karlsruhe, P.O. Box 3640, 76021 Karlsruhe, Germany

**Abstract.** The development of new production technologies for NiTi Shape Memory Alloys (SMAs) is always challenging. Recently, we introduced two powder metallurgical (PM) processing routes involving mechanical activation of elemental powder mixtures and densification through extrusion or forging. Those processes were named Mechanically Activated Reactive Extrusion Synthesis (MARES) and Mechanically Activated Reactive FORging Synthesis (MARFOS). Heat treatments were performed in order to adjust the B2-NiTi matrix composition, yielding a microstructure consisting of a homogeneous dispersion of Ni<sub>4</sub>Ti<sub>3</sub> precipitates embedded in nanocrystalline B2-NiTi matrix. In the present study, we demonstrate the viability of those PM processes for producing NiTi SMAs. With in-situ X-ray diffraction and differential scanning calorimetry it is shown that B2-NiTi matrix undergo a B2↔R↔B19' two-step phase transformation.

## 1. Introduction

NiTi alloys near the equiatomic concentration are the most successful Shape Memory Alloys (SMAs) due to their unique physical and mechanical properties like room temperature ductility, damping effect, corrosion resistance and biocompatibility, which make them attractive for numerous smart engineering and biomedical applications [1].

Intensive effort has been put to adopt alternative production techniques such as powder metallurgy (PM) for manufacturing NiTi SMAs. The main advantage of the PM route is the possibility of producing near-net-shape components and thus avoiding or minimizing the problems associated to the conventional casting methods which are the expensive thermomechanical treatments, machining and associated material losses. However, special attention has to be given to the amount of impurities (especially oxygen and carbon) that are almost unavoidable during PM and casting processing of NiTi. Several conventional PM methods including self-propagating high-temperature synthesis (SHS), reactive sintering, hot isostatic pressure (HIP), hot extrusion and field-activated pressure assisted synthesis have been used for the fabrication of NiTi alloys [2-6].

Our intention is to develop NiTi SMAs by means of two nonconventional PM techniques, which are designated by Mechanically Activated Reactive Extrusion Synthesis (MARES) and by Mechanically Activated Reactive FORging Synthesis (MARFOS). One of the advantages of these techniques is the densification and synthesis of Ni-Ti intermetallics at a relatively low temperature through a controlled reaction [7,8].

The present manuscript reports results of experimental studies focused on the characterization of phase transformations in thermal cycles and microstructures in NiTi alloys having nanosized microstructure prepared by the two original nonconventional PM routes mentioned above. Microstructure is investigated by transmission electron microscopy (TEM) and phase transformations are studied by in-situ X-ray diffraction (XRD) and differential scanning calorimetry (DSC). Although DSC is one of the most commonly used technique to characterize the phase transformation behaviour in SMAs, XRD can detect a smaller volume fraction of the phases compared to thermal methods [9].

---

<sup>a</sup> e-mail: [filipe.neves@ineti.pt](mailto:filipe.neves@ineti.pt)

## 2. Experimental

General sequence of operations involved in MARES and MARFOS processes is shown schematically in Fig.1. The elemental powders were mixed in order to attain the desired composition of Ti-50Ni (at. %). Subsequently, the mixtures were mechanically activated in a vario-planetary mill pulverisette 4. Afterwards, the mechanically activated powders were pressed inside copper cans, which were then placed inside the densification dies. Densification by extrusion (MARES) and by forging (MARFOS) was carried out at 700 °C in a conventional tensile/compression Instron test machine fitted with compression plates. The heating was achieved by induction and the temperature was controlled with a thermocouple in direct contact with the can. For the extrusions the ram moved at a constant speed of 30 mm/min while for the forging experiments a constant ram speed of 6 mm/min and a holding time of 1 min were used. The pressure/ram displacement of each experiment was recorded in a computer (see Fig.1). Subsequent heat treatments, namely, solution and ageing heat treatments were carried out at, respectively, 950 °C/ 24 h and 500 °C / 7 h, both followed by water quenching (WQ).



Fig.1. MARES and MARFOS processes chart.

Characterization of the processed materials was done by XRD (Bruker diffractometer) using  $\text{Cu-K}\alpha$  radiation and TEM (FEI Titan microscope, 300 kV). Oxygen content was determined using a LECO TC-436 analyzer. In-situ XRD and DSC measurements were performed with the purpose of studying the phase transformations occurring in the aged materials. XRD patterns were recorded in a  $2\theta$  range of  $37^\circ$  to  $47^\circ$  at various temperatures between a minimum and maximum of  $-120^\circ\text{C}$  and  $120^\circ\text{C}$ , respectively, using the low temperature chamber attachment TTK-450. The DSC measurements were carried out using a Setaram DSC 92 calorimeter in samples with 50 mg in masses and in a range of temperatures between  $-90^\circ\text{C}$  and  $100^\circ\text{C}$  with heating and cooling rates of  $7^\circ\text{C}/\text{min}$ .

## 3. Results and Discussion

As was previously reported [7], the mechanically activated powders showed a lamellar microstructure consisting of thin alternating lamellae of Ni and Ti. This was the pathway for the decrease of the inter-diffusion distance and hence for the change of reactivity between Ni and Ti. Following the densification by extrusion (in MARES) and by forging (in MARFOS) high density materials were obtained and the layered structure was maintained consisting of thin layers of the intermetallic phases ( $\text{NiTi}$ ,  $\text{Ti}_2\text{Ni}$  and  $\text{Ni}_3\text{Ti}$ ) and of Ni and Ti [7,8]. With the objective of increasing the compositional homogeneity, solution and ageing treatments were performed. The solution treated bulk materials showed quite stable two phase nanostructure with single crystalline NiTi grains and  $\text{Ti}_2\text{Ni}$  grains with substructure of about 30 nm cell size [10]. Following subsequent ageing treatment, a high density of small and evenly distributed  $\text{Ni}_4\text{Ti}_3$  precipitates (labelled as P in Fig.2) were created within the NiTi phase.

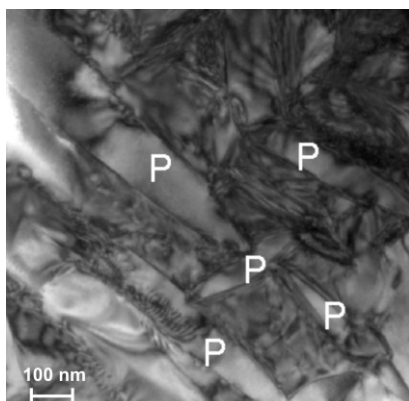
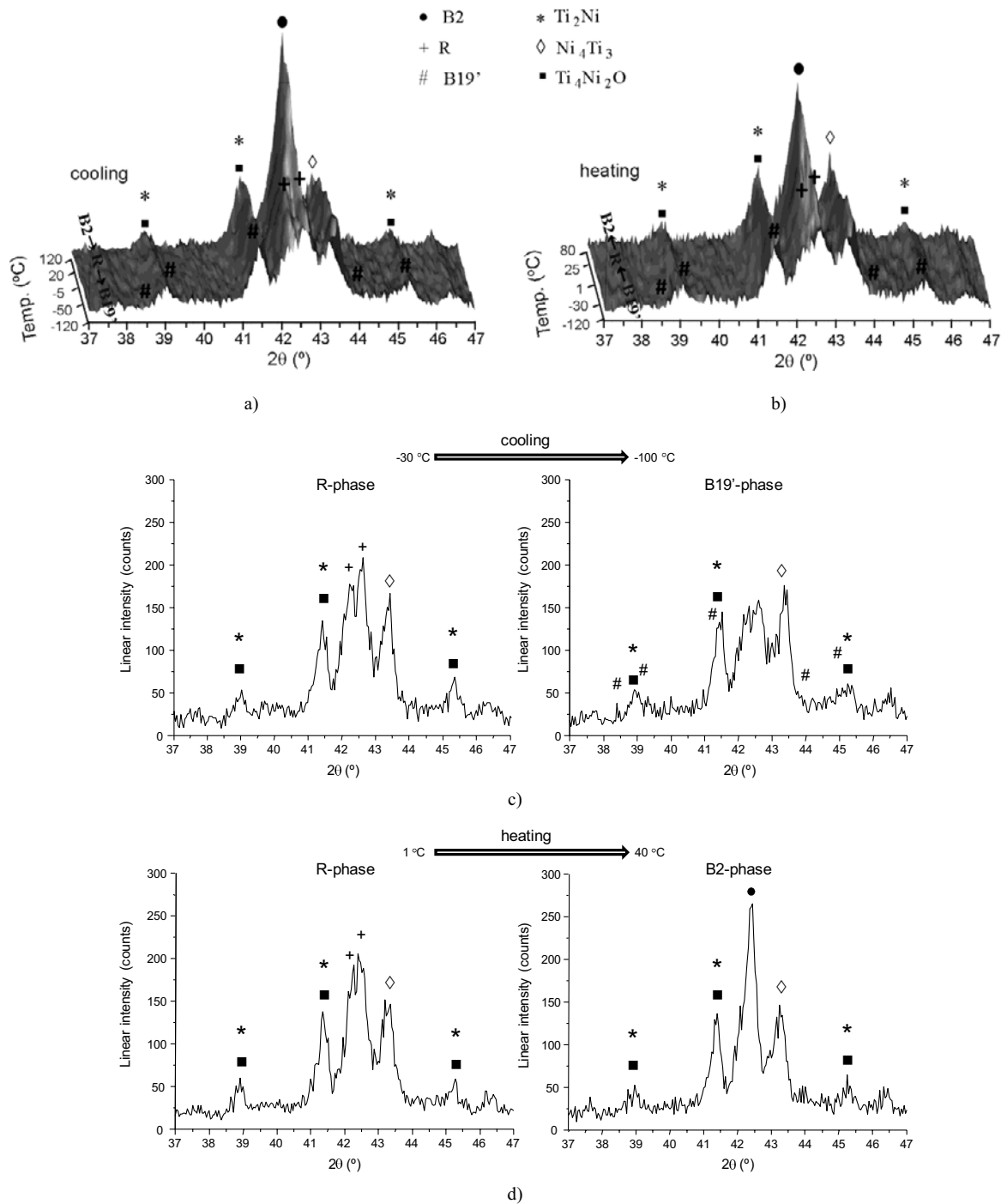
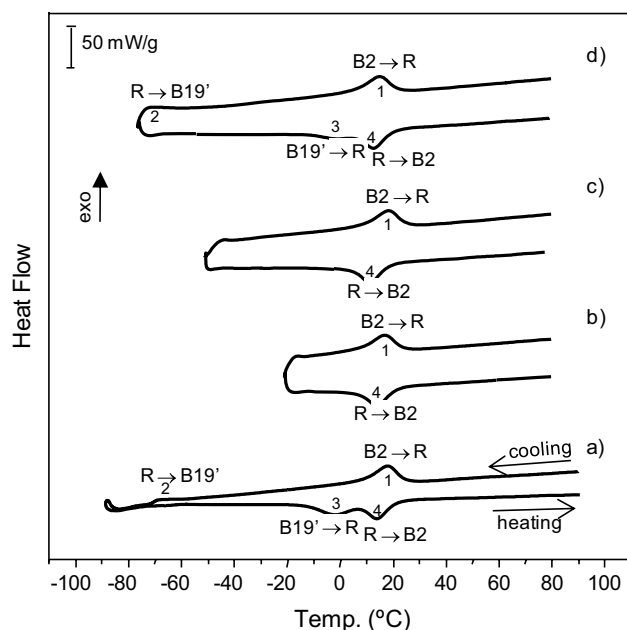


Fig.2. Typical bright field TEM investigation of the MARFOS aged materials.

It is generally accepted that the presence of the metastable  $\text{Ni}_4\text{Ti}_3$  precipitates provides a microstructure which favours the formation of the R-phase prior to the formation of B19'-phase. To identify the nature of the transformation behaviour of MARES and MARFOS aged materials in-situ XRD and partial DSC cycles measurements were carried out on samples of those materials. These two techniques involve controlled cooling and heating to predefined temperatures during which only selected transformations are allowed to occur without triggering other transformations. Fig.3 shows typical in-situ XRD patterns of the aged materials, exemplified for the MARFOS process. In addition, Fig.4 shows typical full and partial DSC cycles of the aged materials, illustrated for the MARES process.



**Fig.3.** Typical in-situ XRD patterns for the MARFOS aged material: overall view of a) cooling from 120 °C to -120 °C and of b) heating from -120 °C to 80 °C; detailed view at c) -30 °C and -100 °C during cooling and at d) 1 °C and 40 °C during heating.



**Fig.4.** Typical DSC measurement of partial transformation cycles for the MARES aged material: a) full cycle and partial cycles up to b) -20 °C, c) -50 °C and d) -75°C.

At room temperature, B2-NiTi, Ti<sub>2</sub>Ni, Ni<sub>4</sub>Ti<sub>3</sub> and Ti<sub>4</sub>Ni<sub>2</sub>O phases were indexed by XRD. The presence of the Ti<sub>4</sub>Ni<sub>2</sub>O was due to relatively high content of oxygen measured by chemical analysis (0.92 ± 0.04 wt %). In fact, Ti<sub>4</sub>Ni<sub>2</sub>O has basically the same structure as the equilibrium Ti<sub>2</sub>Ni phase and therefore they are difficult to distinguish [11].

XRD patterns revealed that, on cooling, the B2 phase was found to be present up to 10 °C, the R phase was identified in the temperature range from 5 °C to -80 °C and the B19' phase from -80 °C up to -120 °C. The XRD patterns of Fig.3c) clearly put in evidence, on cooling, the presence of the R-phase, at a temperature of -30 °C, and of B19'-phase, at a temperature of -100 °C, which in the first case was revealed by the decrease in the intensity and by the split of the peak (1 1 0)<sub>B2</sub> into the peaks of the R-phase, while in the second case by an even bigger decrease of the intensity in the 2theta range of the peak (1 1 0)<sub>B2</sub> and also by the clear indexation of the B19'-phase peaks. On heating, the B19' phase was found to be present up to -20 °C, the R phase was identified in the temperature range from -15 °C to 15 °C and the B2 phase from 20 °C up to 80 °C. Fig.3d) illustrates, on heating, the presence of the R-phase, at a temperature of 1 °C, and of B2-phase, at a temperature of 40 °C, where it is evident the peak (1 1 0)<sub>B2</sub>.

The full DSC cycle (Fig.4a)) shows two peaks on cooling and two peaks on heating. Partial DSC cycle of Fig.4b) (up to -20 °C), indicates that peak 1 on cooling corresponds to peak 4 on heating. This pair of peaks had a small hysteresis of 3.5 °C and so it can be deduced that it must be a B2 ↔ R transformation. Partial DSC cycle of Fig.4c) (up to -50 °C), demonstrates that R-phase have a wide zone of stability during cooling since only peak 1 and peak 4 were again observed. Partial DSC cycle of Fig.4d) (up to -75 °C), revealed peak 2 on cooling and peak 3 on heating. This clearly proves that peak 2 and peak 3 are the forward and the reverse processes of the same transformation, which is the R ↔ B19'. Although, partial DSC cycle of Fig.4d) was stopped at a temperature corresponding to the end of peak 2, it is seen that the intensity of peak 3 is smaller than the correspondent peak observed in the full DSC cycle. From such information, one can deduce that additional cooling is required in order to provide sufficient driving force for the complete R → B19' transformation.

With both techniques, in-situ XRD and DSC, a two-step (B2 ↔ R ↔ B19') phase transformation was then found. Moreover, distinct behaviour on the R ↔ B19' transformation was detected: on cooling, this transformation occurred on a gradual manner and was shifted to very low temperatures, while on heating, the opposite was observed.

## 4. Conclusions

Mechanically Activated Reactive Extrusion Synthesis (MARES) and Mechanically Activated Reactive Forging Synthesis (MARFOS) have been successfully implemented to the production of NiTi shape memory alloys. These processes combine mechanical activation of elemental powder mixtures and densification. The main advantage is the production of highly reactive powders which is responsible for the synthesis and densification at a lower temperature when compared to the conventional PM routes.

Based on in-situ XRD and DSC measurements, the NiTi alloys produced by these two nonconventional PM techniques exhibited a  $B2 \leftrightarrow R \leftrightarrow B19'$  two-step phase transformation. This behaviour was induced by the complex microstructure that was developed during MARES and MARFOS processes. Moreover, the R-phase showed a broad range of stability during the cooling stage of the in-situ XRD and DSC analysis.

F. Neves is supported by an FCT/MCTES Grant (SFRH/BPD/38354/2007). This research was supported by project NAMAMET (more information on the official NAMAMET web site: <http://www2.polito.it/ricerca/namamet/>). F. Neves and F.M. Braz Fernandes acknowledge the pluriannual funding of CENIMAT by FCT/MCTES.

## References

- [1] M.H. Wu, L.McD. Schetky, "Industrial applications for shape memory alloys", The Third International Conference on Shape Memory and Superelastic Technologies, SMST-2000, Pacific Grove, California, 30 April – 4 May 2000, edited by S.M. Russell and A.R. Pelton (ASM, 2001), p. 171
- [2] N. Bertolino, M. Monagheddu, A. Tacca, P. Giuliani, C. Zanotti, U.A. Anselmi, *Intermetallics* **11**, 41 (2003)
- [3] M. Igharo, J.V. Wood, *Powder Metall* **28**, 131 (1985)
- [4] M. Bram, A. Ahmad-Khanlou, A. Heckmann, B. Fuchs, H.P. Buchkremer, D. Stöver, *Mater Sci Eng* **337**, 254 (2002)
- [5] D.G. Morris, M.A. Morris, *Mater Sci Eng* **110**, 139 (1989)
- [6] A.M. Locci, R. Orrù, G. Cao, Z.A. Munir, *Intermetallics* **11**, 555 (2003)
- [7] F. Neves, I. Martins, J.B. Correia, M. Oliveira, E. Gaffet, *Intermetallics* **15**, 1623 (2007)
- [8] F. Neves, I. Martins, J.B. Correia, M. Oliveira, E. Gaffet, *Intermetallics* **16**, 889 (2008)
- [9] J. Uchil, F.M. Braz Fernandes, K.K. Mahesh, *Mater Char* **58**, 243 (2007)
- [10] F. Neves, F.M. Braz Fernandes, I. Martins, J.B. Correia, M. Oliveira, E. Gaffet, T-Y Wang, M Lattemann, J Suffner, H Hahn, submitted to *Smart Materials and Structures* (2009)
- [11] J. Mentz, J. Frenzel, M. Wagner, K. Neuking, G. Eggeler, H. Buchkremer, D. Stöver, *Mater. Sci. Eng. A* **491**, 270 (2008)